JOURNAL OF VIROLOGY, July 1996, p. 4773–4777 Vol. 70, No. 7
0022-538X/96/$04.00+0

The Transmissible Gastroenteritis Coronavirus Contains a Spherical Core Shell Consisting of M and N Proteins

CRISTINA RISCO,[1] INÉS M. ANTÓN,[2]† LUIS ENJUANES,[2] AND JOSÉ L. CARRASCOSA[1]*

Macromolecular Structure Department[1] and Molecular and Cell Biology Department,[2] Centro Nacional de Biotecnología, Consejo Superior de Investigaciones Científicas, Campus Universidad Autónoma, 28049 Madrid, Spain

Received 10 January 1996/Accepted 2 April 1996

Coronaviruses are enveloped RNA viruses involved in a variety of pathologies that affect animals and humans. Existing structural models of these viruses propose a helical nucleocapsid under the virion envelope as the unique internal structure. In the present work, we have analyzed the structure of the transmissible gastroenteritis coronavirus. The definition of its organization supports a new structural model for coronaviruses, since a spherical, probably icosahedral, internal core has been characterized. Disruption of these cores induces the release of N-protein-containing helical nucleocapsids. Immunogold mapping and protein analysis of purified cores showed that they consist of M and N proteins, M being the main core shell component. This surprising finding, together with the fact that M protein molecules are also located in the virion envelope, indicates that a reconsideration of the assembly and maturation of coronaviruses, as well as a study of potential M-protein subclasses, is needed.

Coronaviruses have been described as enveloped, round particles with a prominent layer of surface spikes consisting of complexes of S glycoprotein. These surface structures form the typical "corona" that gives the name to the viral family (5, 22). The viral envelope of coronaviruses contains other glycoproteins, such as the integral membrane protein (M), the small membrane protein (sM), and in some members of the family, the hemagglutinin esterase protein (HE) (9, 13, 21). The nucleocapsid (N) protein is located inside the virion, complexed with the viral RNA (11). Structural models of coronaviruses are based on studies of detergent-treated viral particles and on the analysis of the in vitro interaction of subviral components from disrupted virions. These studies reported the release of helical ribonucleoprotein molecules from mouse hepatitis virus and the 229E strain of the human coronavirus (4, 14). Accordingly, the unique internal structure of coronaviruses is considered to be a helical nucleocapsid constituted by N protein and RNA (5, 21). Sturman et al. (24) proposed that these helical complexes might interact with the intraviral domains of the envelope proteins. The helical RNP of the infectious bronchitis virus has been very difficult to visualize (6, 14, 24), and a previous study (8) failed to release the ribonucleoprotein from transmissible gastroenteritis coronavirus (TGEV). In the present work, we have analyzed the structure of TGEV, a virus that causes severe illness in newborn pigs and that has been the subject of numerous efforts to define the molecular basis of its epidemiology (7). Intact and detergent-treated TGEV virions, which were purified from infected cultures of ST cells (10), have been characterized by negative staining, ultrathin sectioning, freeze fracture, immunogold mapping, and cryoelectron microscopy. In Figure 1 we show representative fields chosen after more than 500 viral particles were studied with each visualization method. Negative staining with 2% uranyl acetate or 2% sodium phosphotungstate was done according to standard procedures (17). Uranyl acetate shows virions (Fig. 1A) that present more extended peplomers when contrasted with sodium phosphotungstate (Fig. 1B). This staining agent sometimes penetrates the viral particles, revealing a compact internal component (Fig. 1C). Ultrathin sections of osmicated virions, obtained as previously described (19), also reveal a continuous structure separated from the envelope that encloses the ribonucleoprotein (Fig. 1D). When TGEV virions are visualized after freeze fracture and platinum-carbon shadowing according to established procedures (18), two different fracture planes are observed. The one that goes along the viral envelope renders large particles (arrows in Fig. 1E), while a second plane along the interior of the virus shows smaller particles (arrowheads in Fig. 1E). The visualization of these smaller structures reveals the presence of an internal shell in TGEV virions.

Cryoelectron microscopy allows the visualization of vitrified, unstained hydrated material (2). This technique avoids the artifacts potentially associated with chemical fixation and staining with heavy metals, allowing the visualization of structures close to their native state. The image of vitrified specimens is thus directly formed by the mass of the different components of the biological structure. The observation of vitrified TGEV virions confirmed the presence of an internal structure inside the virus (Fig. 1F and G). This structure exhibits a polygonal contour (arrowheads in Fig. 1F and G). After 104 viral particles had been measured, a size of 144.8 ± 7.2 nm was calculated for the whole virion (including the extended peplomers), while the internal core had a diameter of 64.5 ± 5.5 nm. These values have to be very close to the real dimensions and clearly differ from the size calculated for the whole virion by negative staining (115.6 ± 10.5 nm), a method that induces a more heterogeneous population of virions. A suspension of latex spheres of homogeneous size (0.0910 ± 0.0058 μm) was used as an internal standard for measurements. A clear gap separated the internal core from the envelope in vitrified virions. The direct visualization of these internal structures was done after a short treatment (3 min at 4°C) of TGEV virions with

* Corresponding author. Mailing address: Centro Nacional de Biotecnología (CSIC), Campus Universidad Autónoma, 28049 Madrid, Spain. Phone: 34-1-5854509. Fax: 34-1-5854506. Electronic mail address: jlcarrascosa@samba.cnb.uam.es.

† Present address: Children's Hospital, Boston, MA 02115.

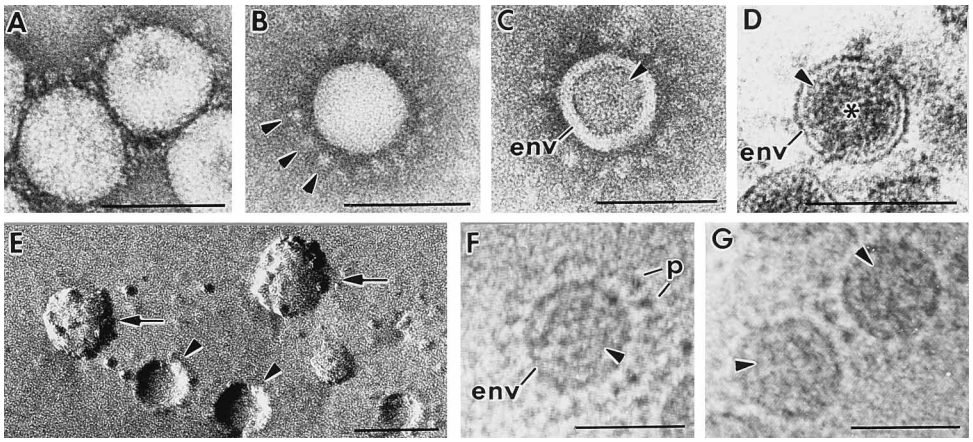

FIG. 1. Structure of purified infective TGEV virions. Negative staining with uranyl acetate (A) or sodium phosphotungstate (B) shows the surface of TGEV particles, whose peplomers are better defined and extended with sodium phosphotungstate (arrowheads). This staining agent frequently penetrates the viral particles (C), revealing an internal structure (arrowhead) separated from the envelope (env). (D) Ultrathin sections reveal the internal organization of these viruses that comprises a continuous layer of material (arrowhead) surrounding the dense ribonucleoprotein (asterisk). (E) Freeze fracture images show two different fracture planes in TGEV virions. One of them goes along the viral envelope (arrows), and the other one reveals a smaller inner shell (arrowheads). (F and G) Cryoelectron microscopy visualization of vitrified TGEV shows particles of homogeneous size that contain an internal structure of geometrical periphery (arrowheads) inside the viral envelope and well-extended peplomers (p). Note the significant gap that separates the internal structure from the envelope. Bars, 100 nm.

two detergents, Triton X-100 (0.025% in phosphate-buffered saline [PBS]) and Nonidet P-40 (NP-40) (0.05% in PBS). The latter was particularly effective, and at the described concentration it removed the envelope, releasing an internal compact structure of proteinaceous nature (Fig. 2A). Immunogold labeling of these structures with specific monoclonal antibodies (MAbs) and a 5-nm colloidal gold conjugate was performed as previously described (16). MAbs specific for M and N proteins (20) clearly reacted with this internal component (Fig. 2B and C). A detectable amount of M-protein molecules remained associated with the disrupted envelopes (Fig. 2B). In contrast, S protein was totally removed since specific MAbs, which pro-

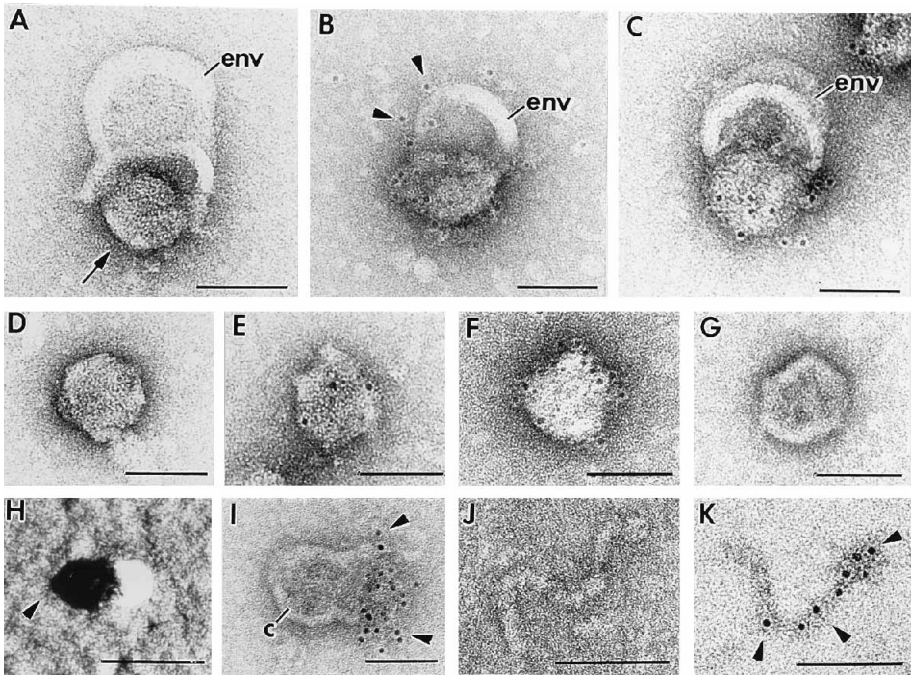

FIG. 2. Release of TGEV internal cores from purified virions by treatment with NP-40. (A) A 3-min incubation at 4°C with NP-40 (0.05% in PBS) induces the disruption of the viral envelope (env), which opens up and releases an internal component of a proteinaceous nature (arrow). Epitopes of M (B) and N (C) proteins are localized on the surface of these internal cores, as revealed by immunogold labeling using specific MAbs. A detectable amount of M molecules remain in the disrupted envelopes (arrowheads in panel B). Higher concentrations of NP-40 (0.25 to 1%) and longer treatments (15 to 30 min) completely removed the viral envelopes, and only particles with a geometrical contour were seen, as visualized by negative staining (D). Immunogold characterization of these particles shows that they react with anti-N (E) and anti-M (F) MAbs, while no signal was obtained with anti-S MAbs (G). (H) Freeze fracture of the particles followed by etching and replication with platinum-carbon showed pointed shadows (arrowhead) consistent with icosahedral structures. (I) Triton X-100-disrupted cores (c) released a material that strongly reacts with anti-N MAbs (arrowheads). This material consisted of helical aggregates that did not react with anti-M MAbs (J) but contained linearly arranged N protein, as indicated by immunogold labeling (arrowheads in panel K). Bars, 70 nm.

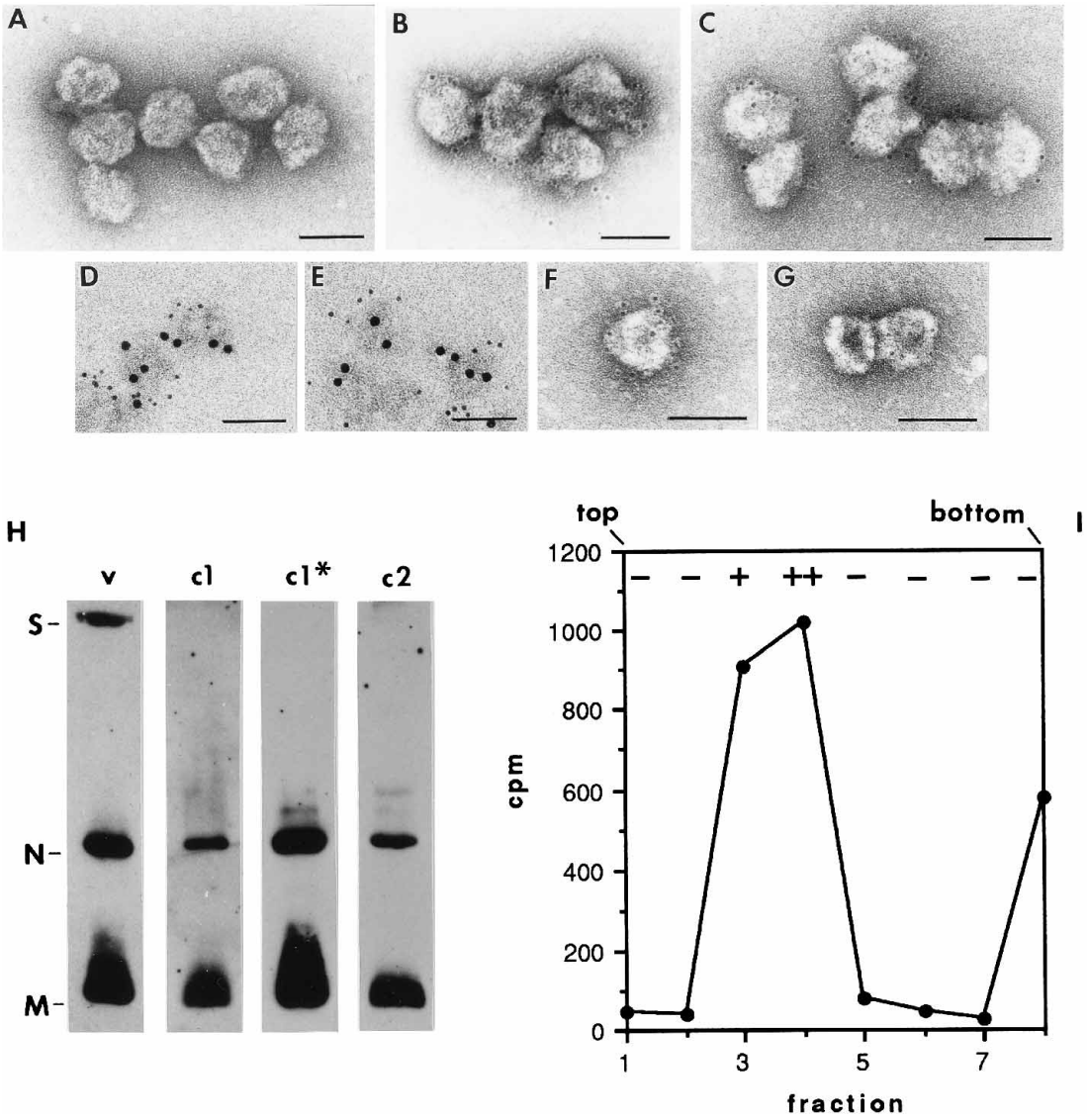

FIG. 3. Characterization of purified TGEV cores. NP-40-treated virions were centrifuged in a sucrose gradient as indicated in the text. (A) The purified cores did not react with anti-S MAbs in immunogold assays, while anti-N (B) and anti-M (C) MAbs clearly bound to their surface. (D and E) Double-labeling of flat-embedded capsids (5-nm gold particles localize N protein, while 10-nm gold corresponds to M protein) showed that the two proteins colocalize in the same structures. In a second purification step (centrifugation in a cesium chloride discontinuous gradient) viral particles appeared as a single band and, although more deteriorated, still preserved their reactivity with anti-M (F) and anti-N (G) MAbs. (H) The protein composition of purified cores was analyzed by Western blot after SDS-PAGE. An anti-TGEV polyclonal antiserum (13) was used. While the intact virions contained S, M, and N proteins (lane v), the cores from fractions 9 (lane c1) and 19 (lane c1*) of the sucrose gradient were constituted by M and N proteins. After being subjected to a cesium chloride discontinuous gradient, the purified cores localized in fractions 3 and 4 had the same protein composition as the sucrose-purified cores (lane c2 corresponds to fraction 4). (I) Viral RNA colocalizes with the purified cores, as confirmed with TGEV containing ^{3}H-RNA. Radioactivity measurements confirmed the presence of labeled viral RNA in the fractions from the cesium chloride gradient that, according to electron microscopy analysis, contained viral cores (+). −, no cores. Bars, 70 nm.

vide a strong signal in intact virions, did not label the disrupted envelopes or the released particles (not shown).

At higher concentrations of NP-40 (0.25 to 1% in PBS) and with longer treatments (15 to 30 min at 4°C) the viral envelopes were totally removed and destroyed, with the release of the internal structure. The released particles had polygonal contours (Fig. 2D) and a diameter of 68.6 ± 4.8 nm, similar to the internal structures visualized in vitrified virions. Immunogold labeling provided a weak signal associated with N protein on the surface of these particles, while M protein covered most of their surface (Fig. 2E and F). No signal associated with S protein was obtained (Fig. 2G). Freeze-etching and shadowing (18) showed pointed (Fig. 2H) or blunt-ended (not shown) shadows consistent with icosahedral structures. When TGEV virions were treated with 0.025% Triton X-100 (3 min at 4°C), similar cores, which clearly reacted with anti-M MAbs, were visualized (not shown). When disrupted by extensive detergent treatment (30 min), these cores released a material that was clearly labeled with anti-N antibodies (Fig. 2I, arrowheads). Once separated from the core, this material was visualized as helical particulated molecules of homogeneous size (Fig. 2J) similar to the ribonucleoprotein molecules described for mouse hepatitis virus and the human coronavirus (14). The helical extended structures did not react with anti-M MAbs (Fig. 2J). Instead, they contained N-protein molecules arranged in a linear pattern as revealed by immunogold labeling (Fig. 2K).

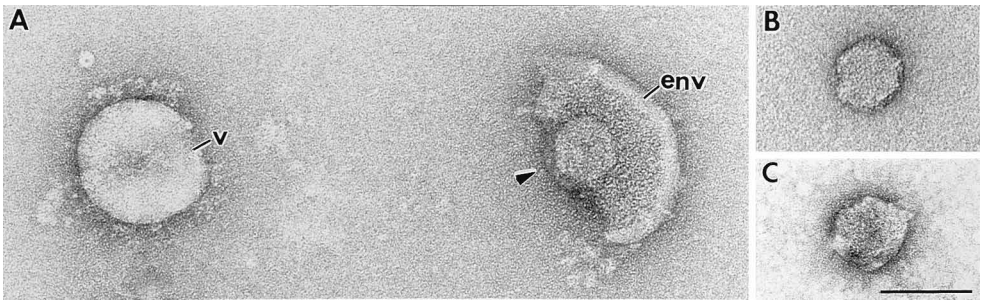

FIG. 4. Subviral structures released by mouse hepatitis virus. (A) Mouse hepatitis virus maintained for 24 h at room temperature spontaneously released internal structures of geometrical periphery (arrowhead). (B) When completely released from the envelopes, the structures were similar to the TGEV internal cores. (C) When incubated for 3 min in 0.1% NP-40 containing 1% glutaraldehyde, these structures were frequently seen. v, intact virion; env, viral envelope. Bar, 70 nm.

TGEV internal cores were purified by centrifugation in a sucrose gradient. NP-40-treated virions (0.5% NP-40, 20 min at room temperature) were centrifuged for 45 min through a linear 15 to 40% sucrose gradient, at 27,000 rpm in a Beckman SW 55Ti rotor at 4°C. The fractions from the gradient were centrifuged for 8 min at 90,000 rpm in a Beckman TLA 120.1 rotor. Pellets were resuspended in PBS containing protease inhibitors (0.1 mM *N*- to syl-L-phenylalanine chloromethyl ketone, 0.1 mM *N*α-*p*-to syl-L-lysine chloromethyl ketone, 1 μg/ml pepstatin A, and 1 mM phenylmethylsulfonyl fluoride) and processed for immunogold and negative staining electron microscopy, polyacrylamide gel electrophoresis in the presence of sodium dodecyl sulfate (SDS-PAGE), and Western blot (immunoblot) (3, 12, 16). Individual cores or small aggregates were found in an intermediate position in the gradient (fraction 9 from the top), while aggregated groups of particles were located at the bottom of the tube (fraction 19). Cores from both fractions were indistinguishable by negative staining and immunogold labeling and were also similar to freshly detergent-released particles (Fig. 3A to C). They did not react with anti-S MAbs (Fig. 3A), moderately reacted with anti-N MAbs (Fig. 3B), and exhibited a stronger signal with anti-M MAbs (Fig. 3C) in immunogold assays. Double immunogold labeling of the cores was done by combining preembedding detection of N protein by specific MAbs and a 5-nm colloidal gold conjugate with postembedding labeling of M protein (detected with a 10-nm colloidal gold conjugate) on sections of flat-embedded particles (17). These experiments showed that M and N proteins were simultaneously located in the same structures (Fig. 3D and E). SDS-PAGE and Western blot analysis showed that while the purified intact virions presented the three major structural proteins, S, M, and N (Fig. 3H, lane v), the cores contained in fractions 9 and 19 from the sucrose gradient consisted of M and N proteins (Fig. 3H, lanes c1 and c1*). The purified cores were submitted to a second centrifugation, in a cesium chloride discontinuous gradient (of 1.15, 1.3, 1.5, and 1.7 g/ml) containing the protease inhibitors indicated above and 0.4 U of the Amersham ribonuclease inhibitor per μl. Centrifugation was performed at 4°C for 45 min at 32,000 rpm in a Beckman TLS-55 rotor. The particles were found in a single band, and their appearance was similar to that in Fig. 3A to C, except that they were slightly deteriorated. They clearly reacted with anti-M MAbs (Fig. 3F), while the signal associated with N protein was weaker (Fig. 3G). The relative amounts of M and N proteins in the cores were maintained, as determined by Western blot analysis after SDS-PAGE (Fig. 3H, lane c2). These data indicate that, after two purification steps, M-protein molecules remain tightly associated with the viral cores in large amounts, covering most of their surface. The purification of cores was also done with a preparation of TGEV labeled with ^{3}H-RNA. This virus was obtained by metabolic labeling of TGEV RNA with [5-^{3}H]uridine followed by virus purification. Infected cultures were incubated in the presence of the radiolabeled precursor, [5-^{3}H]uridine, at a final concentration of 20 μCi/ml from 1 h after virus inoculation until virus was harvested (26 h postinoculation). Purification of the labeled virus was done as previously described (10). When this labeled TGEV was used for purifying the cores, viral RNA colocalized with them in the gradients (Fig. 3I).

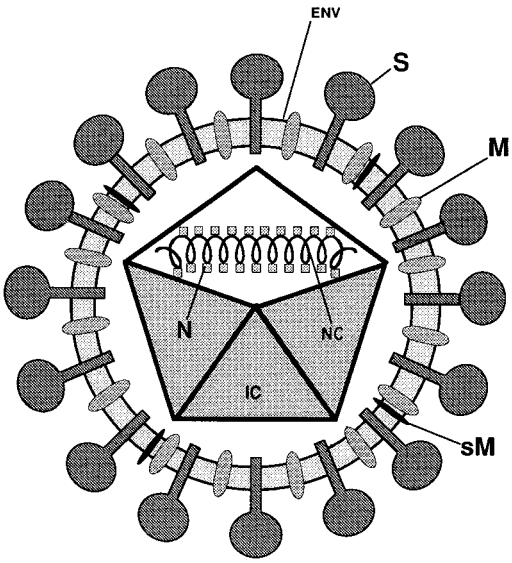

FIG. 5. Structural model of TGEV according to the data presented in this report. ENV, viral envelope, which contains S, M, and sM proteins; IC, internal core (probably icosahedral), consisting of N and M′ (possibly a modified M protein); NC, helical nucleocapsid (ribonucleoprotein consisting of N protein and viral RNA). The details of the interaction between the internal core and the envelope remain to be defined.

We can conclude that TGEV contains a spherical core inside the external viral envelope. The M protein is the main structural component of the core shell, while the N protein also participates as a minor element, probably assembled at specific locations. The core shell contains the (probably helical) nucleocapsid, a structure consisting of the viral RNA and protein N that has been previously described for other coronaviruses (23).

The existence of an internal core shell, something that has not been previously described in coronaviruses, is not exclusive for TGEV, as we have confirmed with virions from the A59

strain of mouse hepatitis virus. These virions, which were purified from infected BALB/3T3 cells (23), spontaneously released an internal core when maintained for 24 h at room temperature (Fig. 4A and B). Incubation with NP-40 (0.05% in PBS for 3 min at 4°C) destroyed the virions, but when 1% glutaraldehyde was present in the detergent solution similar cores were also found (Fig. 4C).

The data presented in this report support the structural model for coronaviruses proposed in Fig. 5. The most striking aspect of this organization is the presence of M protein as the major structural component of the internal core shell. Since M is an integral membrane protein of the virion envelope (1, 16), its presence on the surface of the internal core might be the result of stabilizing interactions from the intravirion domains of M-protein molecules located in the envelope. If these interactions from the envelope do exist, the possibility that the removal of lipids could eventually lead to a massive collapse of M-protein molecules on the internal core cannot be excluded. It is important to note, however, that a significant gap separates the internal core from the envelope in vitrified virions, although focal contacts between both structures could exist (Fig. 1F and G). A second option would be, then, the existence of two M subpopulations at different locations within the viral particle, a possibility suggested by Fig. 2B. In fact, the heterogeneity of M protein as seen with SDS-PAGE, suggests the existence of M subclasses. In infected cells, M-protein molecules could incorporate into viral particles in two different steps or undergo major reorganization in the virion after a single-step incorporation. Since the simultaneous presence of a viral structural protein in two different locations within the virion has not been previously described for other viruses, the assembly process of coronaviruses during morphogenesis should be carefully reconsidered. Studies on the in vivo and in vitro assembly of TGEV are now in progress.

The existence of an internal core shell in coronaviruses cannot be considered a surprising finding, as all positive-strand RNA viruses have a spherical (or icosahedral) core (15). In the particular case of the enveloped positive-strand RNA viruses (togavirus, flavivirus, and arterivirus) the spherical core structures seem to involve a close interaction between protein and RNA. Coronavirus then, would represent a different case, in which the core is built up by an external shell that encloses the helical ribonucleoprotein complex or nucleocapsid. The determination of whether the core shell of coronavirus is truly icosahedral (as expected from our data) demands further studies at higher resolution to check for the presence of the characteristic crystallographic symmetries, with either three-dimensional reconstruction from cryoelectron microscopy (presently under way) or X-ray diffraction from crystals.

This work was partly supported by grant PB91-0109 from the Comisión Interministerial de Ciencia y Tecnología to J.L.C. and by grants from the Comisión Interministerial de Ciencia y Tecnología and the European Union (projects Science and Biotech) to L.E.

REFERENCES

1. **Armstrong, J., H. Nieman, S. Smeekens, P. Rottier, and G. Warren.** 1984. Sequence and topology of a model intracellular membrane protein, E1 glycoprotein, from a coronavirus. Nature **308:**751–752.
2. **Booy, F. P.** 1993. Cryoelectron microscopy, p. 21–54. *In* J. Bentz (ed.), Viral fusion mechanisms. CRC Press, Inc., Boca Raton, Fla.
3. **Burnette, W. N.** 1981. Western-blotting: electrophoretic transfer from sodium dodecyl sulfate-polyacrylamide gels to unmodified nitrocellulose and radiographic detection with radioiodinated protein A. Anal. Biochem. **112:** 195–203.
4. **Caul, E. O., C. R. Ashley, M. Ferguson, and S. I. Egglestone.** 1979. Preliminary studies on the isolation of coronavirus 229E nucleocapsids. FEMS Microbiol. Lett. **5:**101–105.
5. **Cavanagh, D., and The *Coronaviridae* Study Group of the International Committee on Taxonomy of Viruses.** 1994. Revision of the taxonomy of the Coronavirus, Torovirus, and Arterivirus genera. Arch. Virol. **135:**226–237.
6. **Davies, H. A., R. R. Dourmashkin, and R. MacNaughton.** 1981. Ribonucleoprotein of avian infectious bronchitis virus. J. Gen. Virol. **53:**67–74.
7. **Enjuanes, L., and B. A. M. Van der Zeijst.** 1995. Molecular basis of the transmissible gastroenteritis virus epidemiology, p. 337–376. *In* S. G. Siddell (ed.), The Coronaviridae. Plenum Press, New York.
8. **Garwes, D. J., D. H. Pocock, and B. V. Pike.** 1976. Isolation of subviral components from transmissible gastroenteritis virus. J. Gen. Virol. **32:**283–294.
9. **Godet, M., R. L'Haridon, J. F. Vautherot, and H. Laude.** 1992. TGEV corona virus ORF 4 encodes a membrane protein that is incorporated into virions. Virology **188:**666–675.
10. **Jiménez, G., I. Correa, M. P. Melgosa, M. J. Bullido, and L. Enjuanes.** 1986. Critical epitopes in transmissible gastroenteritis virus neutralization. J. Virol. **60:**131–139.
11. **Kapke, P. A., and D. A. Brian.** 1986. Sequence analysis of the porcine transmissible gastroenteritis coronavirus nucleocapsid protein gene. Virology **151:**41–49.
12. **Laemmli, U. K.** 1970. Cleavage of structural proteins during the assembly of the head of bacteriophage T4. Nature **227:**680–685.
13. **Lai, M. M. C.** 1990. Coronavirus. Organization, replication, and expression of genome. Annu. Rev. Microbiol. **44:**303–333.
14. **MacNaughton, M. R., H. A. Davies, and M. V. Nermut.** 1978. Ribonucleoprotein-like structures from coronavirus particles. J. Gen. Virol. **39:**545–549.
15. **Murphy, F. A., C. M. Fauquet, D. H. L. Bishop, S. A. Ghabrial, A. W. Jarvis, G. P. Martinelli, M. A. Mayo, and M. D. Summers (ed.).** 1995. Virus taxonomy, classification and nomenclature of viruses, p. 23. Springer-Verlag, New York.
16. **Risco, C., I. M. Antón, C. Suñé, A. M. Pedregosa, J. M. Martín-Alonso, F. Parra, J. L. Carrascosa, and L. Enjuanes.** 1995. Membrane protein molecules of transmissible gastroenteritis coronavirus also expose the carboxy-terminal region on the external surface of the virion. J. Virol. **69:**5269–5277.
17. **Risco, C., J. L. Carrascosa, A. M. Pedregosa, C. D. Humphrey, and A. Sánchez-Fauquier.** 1995. Ultrastructure of the human astrovirus serotype 2. J. Gen. Virol. **76:**2075–2080.
18. **Risco, C., and P. Pinto da Silva.** 1995. Cellular functions during activation and damage by pathogens: immunogold studies of the interaction of bacterial endotoxins with target cells. Microsc. Res. Tech. **31:**141–158.
19. **Risco, C., C. Romero, M. A. Bosch, and P. Pinto da Silva.** 1994. Type II pneumocytes revisited: intracellular membranous systems, surface characteristics, and lamellar body secretion. Lab. Invest. **70:**407–417.
20. **Sánchez, C. M., G. Jiménez, M. D. Laviada, I. Correa, C. Suñé, M. J. Bullido, F. Gebauer, C. Smerdou, P. Callebaut, J. M. Escribano, and L. Enjuanes.** 1990. Antigenic homology among coronaviruses related to transmissible gastroenteritis virus. Virology **174:**410–417.
21. **Siddell, S. G.** 1995. The Coronaviridae. An introduction, p. 1–10. *In* S. G. Siddell (ed.), The Coronaviridae. Plenum Press, New York.
22. **Spaan, W., D. Cavanagh, and H. C. Horzinek.** 1988. Coronaviruses: structure and genome expression. J. Gen. Virol. **69:**2939–2952.
23. **Sturman, L. S., and K. V. Holmes.** 1983. The molecular biology of coronaviruses. Adv. Virus Res. **28:**35–112.
24. **Sturman, L. S., K. V. Holmes, and J. Behnke.** 1980. Isolation of coronavirus envelope glycoproteins and interaction with the viral nucleocapsid. J. Virol. **33:**449–462.